Dopaminergic Neurons Transplanted Using Cell-Instructive Biomaterials Alleviate Parkinsonism in Rodents

*Maroof M. Adil, Antara T. Rao, Gokul N. Ramadoss, Nicole E. Chernavsky, Rishikesh U. Kulkarni, Evan W. Miller, Sanjay Kumar, and David V. Schaffer**

Cell replacement therapy (CRT) is a promising treatment for degenerative disorders, such as Parkinson's disease (PD). However, CRT is in general hindered by poor graft survival, limited cell dispersion, modest cell integration, and delayed therapeutic efficacy. These challenges need to be addressed to enhance the clinical translation of CRT. Here, key bioactive factors that increase the survival and dispersion of human pluripotent stem cell-derived midbrain dopaminergic (mDA) neurons, the primary type of cells lost in PD, are identified. mDA neurons cotransplanted with survival and dispersion factors within a protective hyaluronic acid hydrogel, optimized for controlled factor release and cell spread, alleviate disease symptoms in PD model rats. Importantly, treatment benefits correlate with increased graft survival, dispersion, and integration. Optimally engineered cell-instructive transplantation platforms thus offer promise for enhancing CRT in PD and potentially a range of degenerative diseases or trauma.

1. Introduction

Parkinson's disease (PD)[1] is a debilitating, progressive, degenerative disorder that affects ≈10 million patients worldwide. PD leads to deterioration of motor and mental function, lacks treatments that offer long-term efficacy, and as a result incurs a major personal and socioeconomic burden[2] with patients experiencing worsening symptoms for the ≈10–20 remaining years of life after disease onset. New treatment strategies are therefore urgently needed.

Cell replacement therapy (CRT), which involves the implantation of cells to reestablish lost functions, is in general a promising treatment strategy for degenerative diseases and traumatic injuries that involve the loss of specific cell populations.[3] For instance, the characteristic loss of striatum-projecting midbrain dopaminergic (mDA) neurons of the substantia nigra is linked to motor dysfunctions in PD.[1] Accordingly, previous clinical trials involving striatal transplantation of fetal-derived dopaminergic tissue showed some improvement in motor function in a subset of patients and thus demonstrated the promise of CRT for PD.[4–6] However, this approach in general has been complicated by graft heterogeneity and limited reproducibility, the challenging supply of transplantable cells, and ethical considerations related to the fetal cell source.[7,8] Fortunately, human pluripotent stem cells (hPSCs), which have the potential for indefinite self-renewal and the capacity to generate most human cell types, are an attractive source of cells for CRT to build upon this early work.[9] The field has made major progress in the efficient and effective generation of defined populations of hPSC-derived mDA progenitors for CRT,[10,11] and steps are underway toward clinical trials in human patients.[12,13] That said, several challenges remain.

First, transplanting heterogeneous populations of progenitor cells may lead to graft overgrowth,[14,15] or movement disorders. Using postmitotic mDA neurons rather than progenitors may avoid this outcome, but these more mature, somewhat delicate cells suffer from low post-transplantation survival[14] due to factors including mechanical stress during harvest and transplantation.[16] Second, dispersion of the graft (i.e., movement of grafted cells apart from one other and the injection site) may enable robust integration with and innervation of host tissues, which is critical for disease alleviation.[17] Additionally, nonuniformly dispersed grafts and the resulting unbalanced dopaminergic activity can induce adverse movement disorders such as dyskinesia in both preclinical and clinical studies.[18,19] Cells are often implanted in multiple locations

Dr. M. M. Adil, G. N. Ramadoss, Prof. S. Kumar, Prof. D. V. Schaffer
Department of Chemical and Biomolecular Engineering
University of California, Berkeley
Berkeley, CA 94720, USA
E-mail: schaffer@berkeley.edu

A. T. Rao, Prof. E. W. Miller, Prof. D. V. Schaffer
Department of Molecular and Cell Biology
University of California, Berkeley
Berkeley, CA 94720, USA

N. E. Chernavsky, Prof. S. Kumar, Prof. D. V. Schaffer
Department of Bioengineering
University of California, Berkeley
Berkeley, CA 94720, USA

R. U. Kulkarni, Prof. E. W. Miller
Department of Chemistry
University of California, Berkeley
Berkeley, CA 94720, USA

Prof. E. W. Miller, Prof. D. V. Schaffer
Helen Wills Neuroscience Institute
University of California, Berkeley
Berkeley, CA 94720, USA

**ADVANCED
SCIENCE NEWS**
www.advancedsciencenews.com

**ADVANCED
FUNCTIONAL
MATERIALS**
www.afm-journal.de

to aid their dispersal across the striatum, but this approach requires multiple injections and may still leave the majority of cells at the injection sites, as mDA neurons are typically not motile.[20] Exogenous cues may thus be necessary to promote graft dispersion. Finally, successful grafts must currently mature and integrate for several months within animal models before achieving the functionality required to alleviate disease symptoms,[10,11] and an analogous delay occurs in PD patients, who continue to experience motor and behavior dysfunction for years after cell transplantation before treatment benefits are realized.[21,22] For all of these reasons, approaches to enhance post-transplantation survival and dispersion of grafted neurons and thereby improve and accelerate treatment efficacy may benefit clinical translation of CRT in PD.

Harnessing engineered biomaterials for transplantation could potentially enhance the postimplantation survival, dispersion, and integration of postmitotic mDA neurons to enable safe, rapid, overgrowth-free CRT. First, biomaterial scaffolds may physically protect against mechanical and inflammatory stress during and post-transplantation.[23] Additionally, incorporation of key biochemical cues within the biomaterial scaffold—for example, neurotrophic factors to promote cell survival or motogenic factors to encourage cell migration—may both further enhance post-transplantation cell survival and aid in the dispersion of fragile, generally immotile postmitotic neurons. Such cue-mediated dispersion of stem cell-derived cells has not previously been attempted in a cell replacement therapy, and this may be a particularly valuable strategy to promote functional graft integration in the CNS.

Here, we utilize cell-instructive biomaterial platforms to enhance the post-transplantation survival and dispersion of human embryonic stem cell (hESC)-derived mDA neurons. Specifically, we experimentally identified factors that dispersed hESC-derived mDA neurons and incorporated these factors into a hyaluronic acid (HA) based hydrogel to build a dispersion-inducing transplantation platform. Following mDA neuron generation in a scalable, thermoresponsive hydrogel,[24] cells were encapsulated into these hydrogels, implanted into PD model rats, and alleviated disease symptoms. Importantly, this symptomatic amelioration correlated with significantly increased mDA neuronal survival, dispersion, and host-tissue innervation. This transplantation strategy may thus facilitate clinical translation of regenerative therapy for PD, and additionally holds promise for CRT in other diseases.

2. Results

2.1. Motogenic Factors Disperse hESC-Derived mDA Neurons on 2D Surfaces

We first identified biological factors that could increase cell motility and dispersion of hESC-derived neurons (**Figure 1**a). Several candidate factors generally associated with cell motility, migration, or axonal projection were selected for analysis: (1) scatter factor, or hepatocyte growth factor (SF/HGF),[25] (2) fibroblast growth factor (FGF-2),[26] (3,4) Ephrin-B1 and Ephrin-B2,[27] and (5) glial derived neurotrophic factor (GDNF).[28] Ephrins in particular are well-known for their role

in axonal guidance during central nervous system development.[29] Furthermore, string pathway analysis, an open-source database-linked tool to assess molecular function based on literature evidence, confirmed that these molecules were broadly associated with neuronal projection, axon guidance, and cell migration (Table S1, Supporting Information).

We investigated whether these factors could disperse hESC-derived postmitotic mDA populations, initially on 2D laminin-coated surfaces. H1 hESCs were differentiated into mDA neurons, using the fully defined and scalable system based on the thermoresponsive poly(N-isopropylacrylamide)-*co*-polyethylene glycol (PNIPAAm-PEG)-material we recently reported[24] (Figure 1b). Notably, this approach generated mDA neurons with elevated levels of EN1, which has been linked to increased graft survival,[11] and FOXA2, which is associated with mDA development and long-term graft survival.[30,31] After 25 d of differentiation within the PNIPAAm-PEG gel, mDA clusters expressed FOXA2, LMX1A, and TH, demonstrating a region-specific dopaminergic phenotype (Figure 1c–e).[10] Specifically, our previous analysis showed that ≈80% of these cells express FOXA2 and LMX1A (demonstrating a floor-plate-derived midbrain neural fate), ≈70% express the pan-neuronal marker TUJ1, and ≈40% express TH.[24] Subsequently, clusters were isolated and seeded on laminin-coated 2D surfaces for motility experiments. In an initial screening experiment, using Cell Profiler software (as depicted in Figure S1, Supporting Information), we identified Ephrin-B2 (10 ng mL^{-1}), HGF (20 ng mL^{-1}), and GDNF (100 ng mL^{-1}) as the most potent dispersion factors for mDA neurons, as they dispersed cells to a 5–10-fold greater extent than the other factors tested (Figure 1f). Factor concentrations used were similar in order of magnitude to values previously shown to disperse other neural cells.[25,26,28] We additionally verified that the dispersion factors did not affect the total number of cells (Figure S2, Supporting Information), for example, through altering proliferation rates or cell viability.

2.2. GDNF, Ephrin-B2, and HGF Disperse hESC-Derived mDA Neurons Encapsulated in 3D Hyaluronic Acid Gels In Vitro

To determine whether the results observed on 2D translated into a less spatially constrained and more brain-mimetic 3D environment, and to develop a transplantable platform to induce cell dispersion in vivo, we next investigated cell dispersion within a biomaterial. Specifically, we coencapsulated dispersion factors and cells in a transplantable biomaterial (**Figure 2**a) based on HA—a base material that has previously been used as both in vitro tissue models and cell transplantation scaffolds.[23,32,33] As a first step, we demonstrated that HA hydrogels functionalized with RGD, a cell adhesive peptide,[34] and heparin, a glycosaminoglycan with high affinity for key neurotrophic factors,[35–37] supported culture of D25 hESC-derived mDA neurons initially generated in PNIPAAm-PEG (Figure 2b,c). Of note, both RGD and heparin have been extensively used before for their adhesive and factor-binding properties, respectively, to functionalize biomaterials.[34,38] The coexpression of TH, FOXA2, and LMX1A after 10 d in the HA-based biomaterial (D35) importantly demonstrates maintenance of a midbrain-specific dopaminergic phenotype.[10]
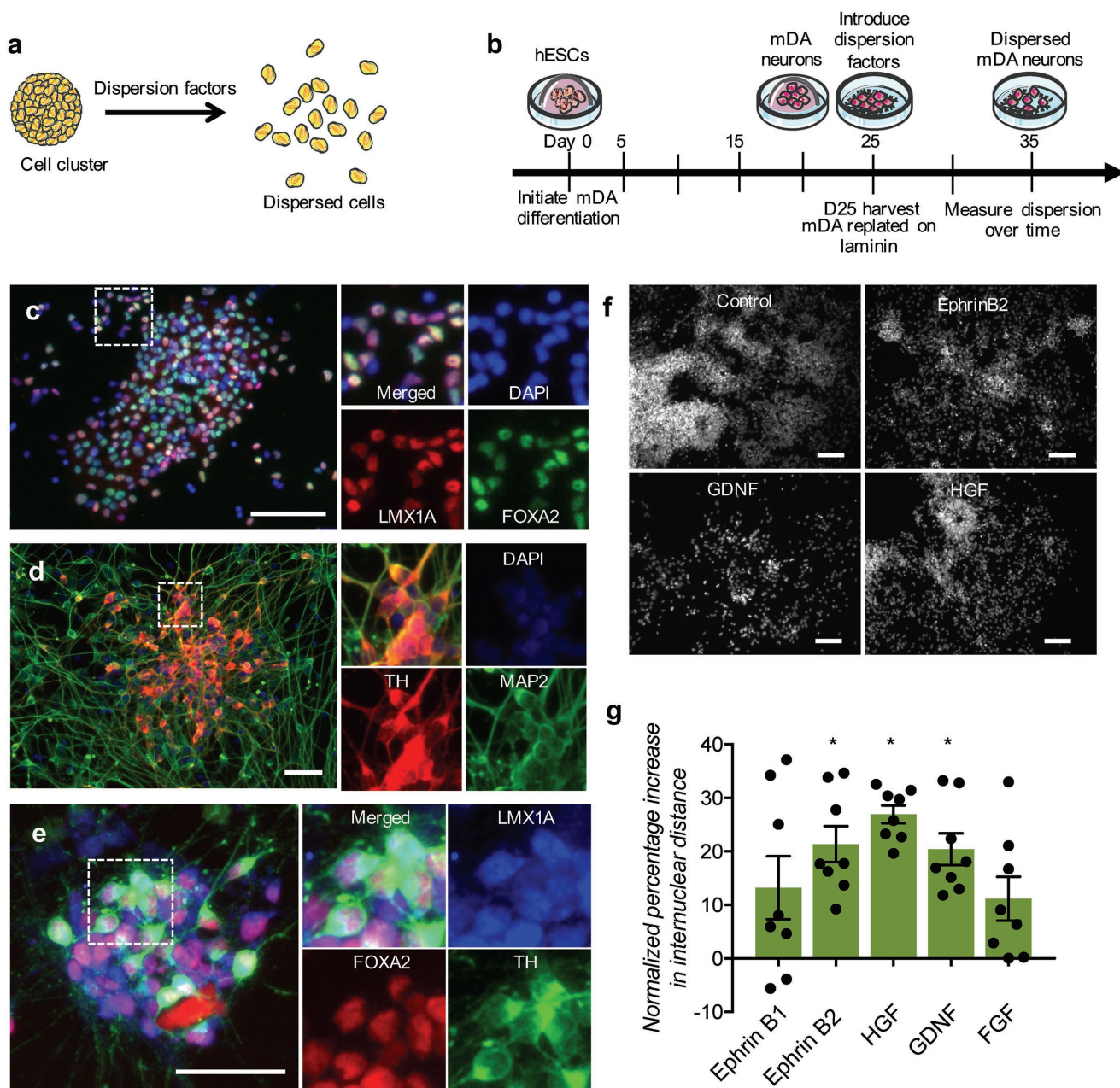
Figure 1. hESC-derived mDA neurons are dispersed by biological cues in vitro. a) Schematic for cell dispersion concept. b) Schematic for generating hESC-derived mDA neurons in thermoresponsive hydrogels, followed by investigating the effect of soluble dispersion factors on 2D laminin-coated surfaces. Representative immunocytochemistry of D25 hESC-derived mDA neurons showing coexpression of c) LMX1A (red) and FOXA2 (green), with nuclei labeled with DAPI (blue); of d) TH (red) and MAP2 (green), with nuclei labeled with DAPI (blue); and of e) TH (green), FOXA2 (red), and LMX1A (blue). Scale bars are 50 µm. f) Representative images of DAPI-labeled nuclei for mDA neurons incubated with soluble Ephrin-B2, HGF, or GDNF. Scale bars are 200 µm. g) Percentage increase in internuclear distances for hESC-derived mDA neurons treated for 2 d with soluble dispersion factors on 2D laminin-coated surfaces, relative to internuclear distances for untreated controls. Data are presented as mean ± SEM ($n = 8$ experiments, analyzing 5200 ± 100 cells per condition). * indicates $p < 0.05$ for Student's unpaired t-test with respect to control untreated cells.

Next, we investigated whether soluble GDNF, Ephrin-B2, and HGF added to culture medium at levels that were active in 2D (Figure 1e) could disperse mDA neurons encapsulated in the 3D HA biomaterial. Since material properties such as stiffness (Figure 2d, and Figure S3a, Supporting Information) can affect migration in 2D[39] and 3D,[40] material crosslinking and thus stiffness were also varied. Ephrin-B2 (10 ng mL^{-1}), GDNF

(100 ng mL^{-1}), and HGF (20 ng mL^{-1}) dispersed HA-encapsulated neurons (Figure 2e,f), as well as enhanced ($p < 0.0001$) neurite outgrowth (Figure 2e,g), including TH$^+$ neurites (Figure S3b–d, Supporting Information), with important implications for promoting graft–host tissue connectivity.[17] Furthermore, HA-based hydrogels with the highest initial storage moduli tested (≈750 Pa) resulted in the highest levels of
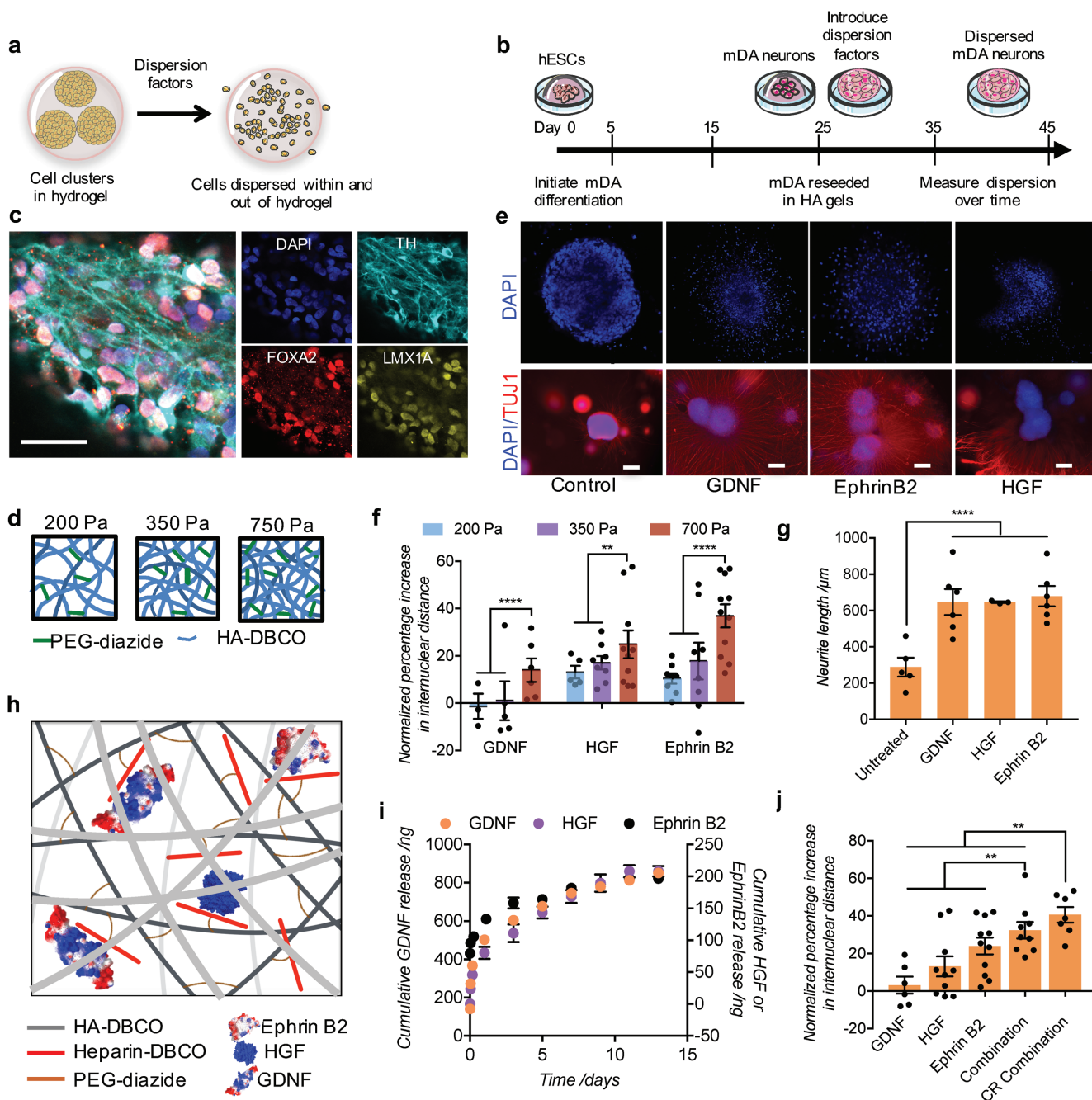
Figure 2. hESC-derived mDA neurons are dispersed by biological cues in 3D HA hydrogels. a) Schematic for cell dispersion concept. b) Schematic for investigating the effect of dispersion factors in 3D. c) Representative immunocytochemistry image showing HA-encapsulated D35 hESC-derived mDA neurons coexpressing TH (cyan), FOXA2 (red), and LMX1A (yellow), with nuclei labeled in blue. Scale bar is 100 µm. d) Schematic for generating HA gels with varying stiffness. e) Representative images showing mDA neurons treated with dispersion factors for 10 d in 750 Pa HA hydrogels. Top panels: Higher objective confocal images showing dispersed DAPI-labeled nuclei. Bottom panels: Lower objective images showing neurite extension, with cells stained for TUJ1 (red) and with DAPI (blue). Scale bar is 200 µm. f) Percentage increase in internuclear distances for hESC-derived mDA neurons treated for 10 d with soluble dispersion factors in HA gels of stiffness 200 Pa (orange), 350 Pa (blue), or 750 Pa (purple), relative to internuclear distances for untreated controls. Data are presented as mean ± SEM ($n > 3$). g) Average neurite length in hESC-derived mDA cultures treated with soluble dispersion factors in 750 Pa HA gels. Data are presented as mean ± SEM ($n \geq 3$). h) Schematic for dispersion factors GDNF, HGF, and Ephrin-B2 incorporated within HA gels. i) Release kinetics of dispersion factors GDNF (orange), HGF (purple), and Ephrin-B2 (black) from 750 Pa HA gels. Data are presented as mean ± SEM ($n = 3$). j) Percentage increase in internuclear distances for hESC-derived mDA neurons treated with soluble dispersion factors individually or in combination for 10 d in 750 Pa HA gels (Combination), or for hESC-derived mDA neurons coencapsulated with all dispersion factors in 750 Pa HA gels (CR Combination) for 10 d, relative to internuclear distances for untreated controls. Data are presented as mean ± SEM ($n > 6$ experiments). ** indicates $p < 0.01$ and **** indicates $p < 0.0001$ for one-way ANOVA with Tukey's test for multiple comparison.

dispersion (Figure 2f), potentially due to increased cell traction in a stiffer material.[39] Stiffnesses higher than 750 Pa were not tested due to limitations in material injectability. In sum, more cells in the higher stiffness gels were dispersed over longer distances in the presence of the dispersion factors (Figure S3e, Supporting Information).

Next, we devised a platform that could continuously release encapsulated factors over at least two weeks to allow dispersion following transplantation in vivo. GDNF, HGF, and Ephrin-B2 were incorporated during crosslinking of the HA-based hydrogels, and factor release was quantified over two weeks via ELISA. These dispersion factors (which have solvent-accessible, positively charged domains[41–43]) have the potential to be both electrostatically bound to heparin and physically encapsulated within the hydrogels (Figure 2h), leading to subsequent slow release from the material via diffusion and hydrogel degradation.[44] HGF and GDNF may additionally interact with heparin.[45,46] Encapsulating 0.5 µg Ephrin-B2, 0.5 µg HGF, and 1 µg GDNF into 30 µL HA-based hydrogels led to an initial burst release followed by slower release rates of ≈3 ng mL^{-1} d^{-1} Ephrin-B2, ≈13 ng mL^{-1} d^{-1} HGF, and ≈30 ng mL^{-1} d^{-1} GDNF, respectively (Figure 2i).

Next, hESC-derived mDA progenitors were incorporated into these HA-based hydrogels, factors were added either during cell encapsulation or solubly to culture medium after cell encapsulation, and cell dispersion was measured. Individual factors induced dispersion (3% for GDNF, 10% for HGF, or 24% for Ephrin-B2 relative to untreated controls), and the dispersive effect was more pronounced ($p < 0.0001$) when factors were combined (Combination, Figure 2j). Furthermore, even higher ($p < 0.0001$) dispersion (35% increase relative to untreated controls) was observed when all factors were coencapsulated with cells (CR Combination, Figure 2j).

2.3. hESC-Derived mDA Clusters Encapsulated in Dispersive HA Gels Improve Function in PD Model Rats

We next investigated whether hESC-derived mDA cells coencapsulated with dispersive factors in HA-based hydrogels could alleviate disease symptoms in a rat model of PD. mDA neurons were generated (1) on common 2D platforms (Matrigel) (2D group, or 2D), (2) in 3D PNIPAAm-PEG and prepared as a suspension (3D group, 3D),[24] (3) in 3D PNIPAAm-PEG and encapsulated in HA gels without factors (3D + gel group, 3DG), or (4) in 3D PNIPAAm-PEG and encapsulated in HA hydrogels with factors (3D + gel + factors group, 3DGF). In addition, we hypothesized that the supportive environment provided by the functionalized HA gels would allow us to attempt transplanting considerably fewer cells, 100 000 postmitotic mDA neurons compared to 150 000–450 000 cells generally transplanted in these models,[10,47–50] and have them survive and functionally engraft. 100 000 cells in these four groups were thus striatally transplanted in 6-OHDA unilesioned PD model rats (**Figure 3**a), while in parallel using phosphate buffered saline (PBS) (sham) and cell-free gel with factors (gel+factors group, gel) as controls. At the time of transplantation (D25 of differentiation), the fraction of TH$^+$ cells generated on 2D and in 3D were 20 and 35%, respectively, consistent with our previous report.[24]

After transplantation, we monitored animals monthly for five months in a blinded manner using two standard tests for motor function in PD: apomorphine-induced rotation[51] (rotation tests; Figure 3b) and the cylinder test for forelimb akinesia[52] (Figure 3c). Briefly, in the rotation test, intraperitoneal injections of a dopamine agonist such as apomorphine stimulates the sensitized dopamine receptors in the lesioned striatum of unilaterally lesioned PD models, leading to contralateral (with respect to the lesioned side) rotations that serve as a quantitative measure of pathology. In the cylinder test, quantifying reduced usage of the contralateral forelimb in unilaterally lesioned animals offers an additional measure of disease.

The 2D cell cohort did not improve in the rotation tests relative to sham surgery animals, and only showed increased usage of the contralateral forelimb at the 12-week time-point (Figure 3b,c). Consistent with prior reports,[10,47,48] higher cell numbers transplanted at an earlier time-point (of differentiation) may be needed to achieve more than the transient motor improvement observed here with 2D cells. In contrast, as early as 4–8 weeks post-transplantation we observed reduced ($p < 0.05$) apomorphine-induced rotations for the 3D, 3DG, and 3DGF cohorts (Figure 3b) demonstrating rapid alleviation of disease symptoms. However, at subsequent time-points 3D-differentiated cells without material (3D) performed poorly on the rotation test and showed increased contralateral forelimb usage only at 12 weeks after transplantation (Figure 3c). For 3DG, however, improvement in forelimb akinesia was maintained until 16 weeks after transplantation, but performance on the rotation test deteriorated sooner. In stark contrast, 3DGF demonstrated improved motor function for the entire duration of the study, outperformed all the other treatment groups by the end of five months, and achieved nearly complete recovery of contralateral forelimb function after only eight weeks post-transplantation (Figure 3b,c). Furthermore, these results persisted for the duration of the five-month experiment (Figure S4, Supporting Information). Since gel+factors without cells (gel) showed no benefit at any time-point, the combined delivery of mDA neurons and factors coencapsulated in HA-based hydrogels was key in alleviating disease symptoms in this PD rat model.

Finally, amphetamine-induced rotation[54] (Figure S5a, Supporting Information) and stepping tests[54] (Figure S5b, Supporting Information) analysis of motor function five months post-transplantation confirmed the superior performance of 3DGF.

2.4. Functionalized HA Hydrogels Enhanced Post-Transplantation Survival, Phenotype Maintenance, Integration, and Dispersion of 3D Generated hESC-Derived mDA Neurons

We histologically examined the various treatment groups five months post-transplantation, specifically graft survival, cell phenotype, neuronal connectivity, and dispersion. Surviving human nuclear antigen-positive (HNA$^+$) striatal grafts were seen in all cell-based treatment groups (**Figure 4**a–d). On average, ≈1500 HNA$^+$ and ≈2300 HNA$^+$ cells survived for 2D and 3D, respectively, out of 100 000 cells transplanted (Figure 4e). In contrast, we noted higher survival in groups with cells encapsulated in HA-based hydrogels (i.e., 3DG and 3DGF), with ≈6100 and
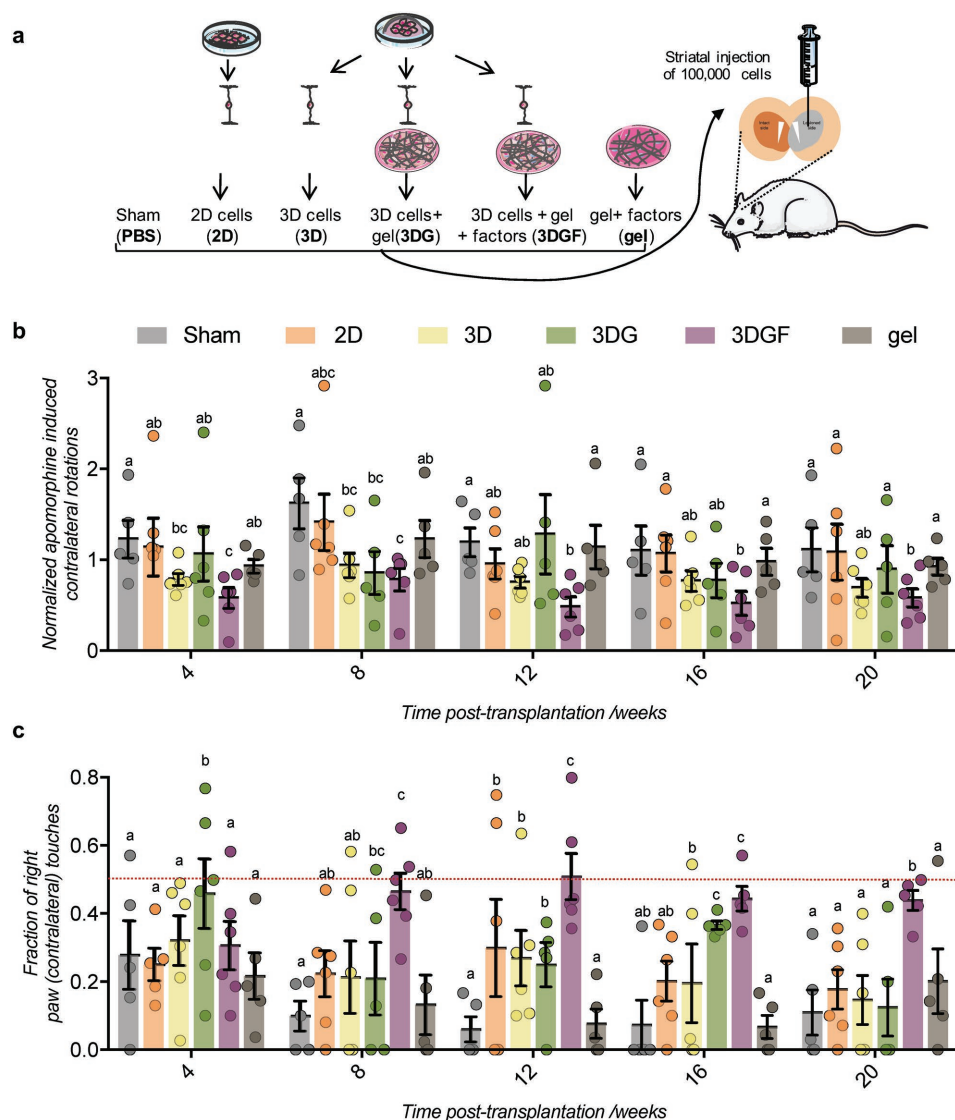
**ADVANCED
SCIENCE NEWS**
www.advancedsciencenews.com

**ADVANCED
FUNCTIONAL
MATERIALS**
www.afm-journal.de

Figure 3. Transplantation of hESC-derived mDA neurons coencapsulated with dispersion factors into 6-OHDA unilesioned PD model rats rapidly alleviates disease symptoms and outperforms alternative treatment groups. a) Schematic representing the six different groups used for in vivo experiments. b) Apomorphine-induced contralateral rotations; rotation data for each animal are normalized to its respective pretransplantation rotation value. c) Fraction of right (contralateral) paw touches in the cylinder test. Dashed red line shows level for full recovery. Groups presented here are: sham (gray), 2D (orange), 3D (yellow), 3D gel (green), 3D gel + factors (purple), and gel (olive). Data are presented as mean ± SEM for $n = 6$ animals for each treatment group, and $n = 5$ animals for controls. Statistical analysis was performed separately for each time point using one-way ANOVA with Tukey's test for multiple comparisons; group means within each time point sharing a letter label are part of the same statistical group with $p > 0.05$; group means within each time point that do not share a letter label are statistically different $p < 0.05$.

≈4800 HNA$^+$ cells surviving respectively out of 100 000 cells transplanted (Figure 4e).

Importantly, we found the highest fraction of TH$^+$/FOXA2$^+$ neurons, the cells relevant for disease alleviation,[10] in 3DGF (Figure 4f–i, and Figure S6, Supporting Information). Specifically, out of the surviving cells, 75% were TH$^+$ in the 3DGF group, significantly and substantially higher ($p < 0.05$) than the 19% TH$^+$, 20% TH$^+$, and 13% TH$^+$ cells observed for the 2D, 3D, and 3DG groups, respectively. The significant difference in the fraction of TH$^+$ cells between 3DG and 3DGF suggests that inclusion of neurotrophic dispersion factors was crucial for long-term preservation of the mDA phenotype

in vivo. The maturation and maintenance of region-specific phenotype within the 3DGF graft was further confirmed by the coexpression of TH and GIRK2, a hallmark potassium channel protein marker of A9-type mDA neurons (Figure S7, Supporting Information). Additionally, we found <1% Ki67$^+$ proliferative human cells five months post-transplantation, thereby demonstrating a lack of graft proliferation consistent with a safer graft (Figure S8a, Supporting Information). We also found no immune response around the graft area at this time-point, with similar levels of Iba1$^+$ host microglia and no CD68$^+$ host macrophages (Figure S8b, Supporting Information) compared to an uninjured rat striatum (Figure S8c, Supporting
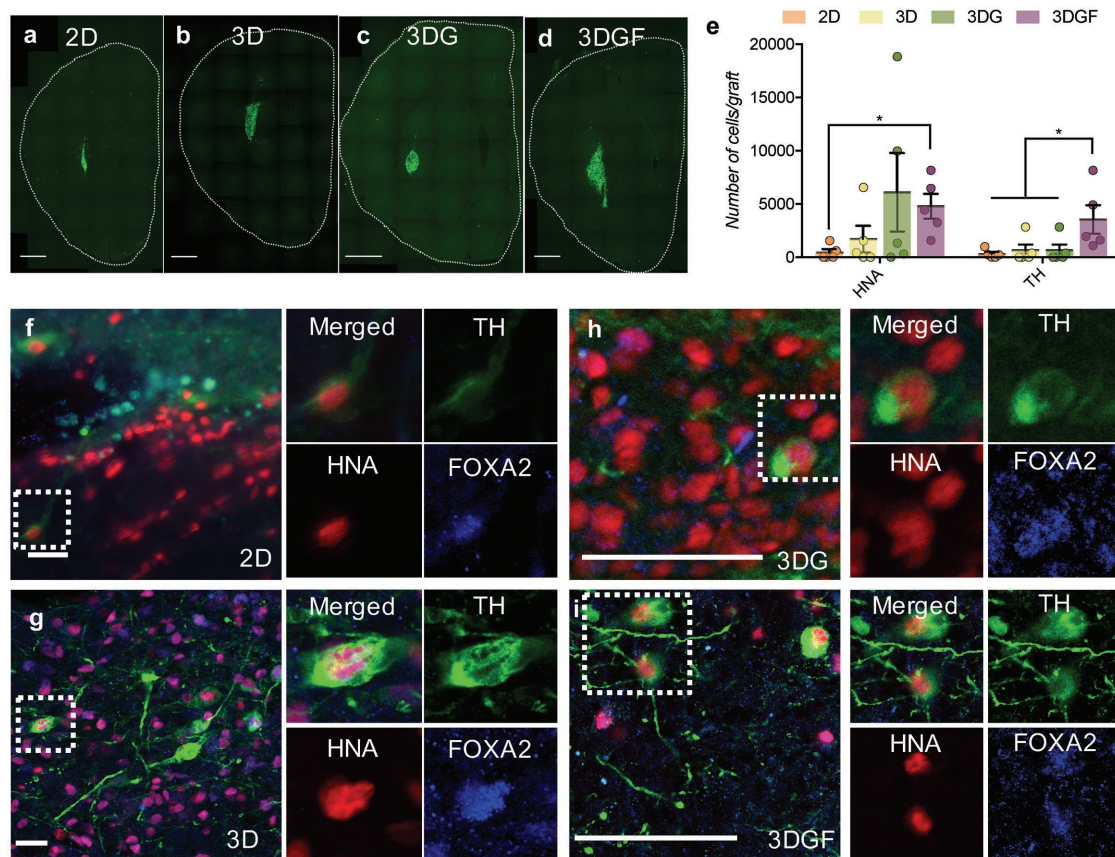
Figure 4. HA hydrogels with incorporated dispersion factors mediated increased survival and phenotype maintenance of cotransplanted hESC-derived mDA neurons at 20 weeks post-transplantation relative to other treatment groups. a–d) Representative images of HNA^{+} cells (green) in surviving striatal grafts for each of the treatment groups. Scale bars are 500 µm. e) Quantification through immunohistochemistry showing the average number of total and TH^{+} cells surviving for each treatment group: 2D (orange), 3D (yellow), 3DG (green), and 3DGF (purple). Data are presented as mean ± SEM from $n = 5$ animals per group. * indicates $p < 0.05$ for one-way ANOVA with Dunnett's test for multiple comparisons. Absence of brackets denotes no statistical significance, with $p > 0.05$. f–i) Representative images of HNA^{+} cells (red) within grafts coexpressing TH (green) and FOXA2 (blue) for each of the treatment groups 2D, 3D, 3DG, and 3DGF, respectively. Scale bars are 50 µm.

Information). In contrast, higher numbers of microglia and macrophages were seen in the suspension cell grafts without scaffolds (Figure S8d, Supporting Information).

We next investigated whether the cell-instructive biomaterial led to increased dispersion and innervation in vivo. First, measuring internuclear distances of grafted cells indeed showed that incorporating dispersion cues (3DGF) increased ($p < 0.005$) dispersion relative to all other treatment groups (**Figure 5**a,b, and Figure S9, Supporting Information). Specifically, 3DGF showed an average internuclear distance of 14 µm, which is 1.5–2-fold higher compared to unaided migration in the other treatment groups (Figure 5b). At a gross morphological level, 3DGF grafts were observed to span across multiple histological sections (Figure S10, Supporting Information), with dense TH neurite innervation at the graft periphery (Figure S11, Supporting Information). Specifically investigating the effect of dispersion factors on host tissue innervation, NCAM (**Figure 6**a–f) and STEM121 (Figure 6g–j) staining demonstrated denser levels of neurite outgrowth at the 3DGF graft periphery relative to 3DG. Importantly, we also found 3DGF grafts to be significantly more spread out relative to 3DG ($p < 0.05$) (Figure 6k).

To promote functional recovery, grafted cells should ideally form synaptic connections with the surrounding neuronal architecture,[17] emulating the synaptic connections of endogenous nigral projection neurons with their striatal targets.[55,56] In accordance, we noted human TH^{+} neurons expressing human synaptophysin (hSYP) in all treatment groups (Figure 5c, and Figure S12a–c, Supporting Information). This synaptophysin expression also occurred in close proximity to DARPP32^{+} medium spiny neurons (MSNs) in the 3DGF group, suggesting connectivity between grafted neurons and the surrounding striatum (Figure 5d). Importantly, a higher level of hSYP was detected in the graft periphery for 3DGF grafts, relative to the other treatment groups (Figure 5d,e, and Figure S12d–f, Supporting Information), indicating increased synapse formation. Rapid synaptic integration may be facilitated by higher maturity of transplanted cells. Using voltage-sensitive fluorescent dyes to monitor spiking activity[57]—a hallmark of neuronal maturation—we observed that 80% of 3D-generated neurons fired action potentials at D31 of differentiation in vitro (Figure S13, Supporting Information). Such functionally mature neurons may integrate with the host neuronal architecture faster, and lead to rapid alleviation of disease symptoms. Thus, the
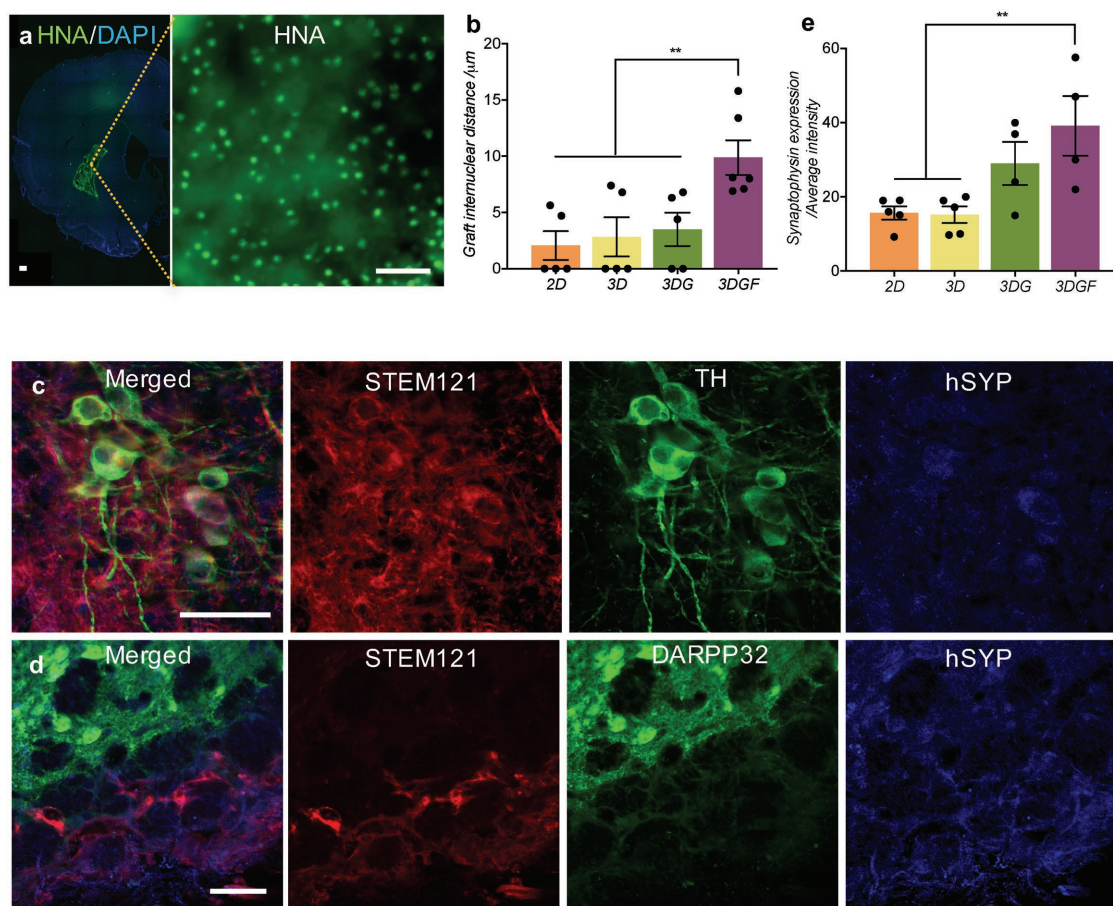
**ADVANCED
SCIENCE NEWS**
www.advancedsciencenews.com

**ADVANCED
FUNCTIONAL
MATERIALS**
www.afm-journal.de

Figure 5. hESC-derived mDA neurons transplanted with dispersive hydrogels demonstrate enhanced synaptic integration and dispersion at 20 weeks post-transplantation. a) Representative images of dispersed HNA stained human nuclei (green) for 3DGF. Scale bars 50 µm. b) Average internuclear distance among grafted cells for each of the different treatment groups: 2D (orange), 3D (yellow), 3DG (green), and 3DGF (purple). Data are presented as mean ± SEM for n = 5 animals/group. c) Representative immunohistochemistry images showing STEM121-labeled human cells coexpressing TH (green) and hSYP (blue). d) Representative images showing STEM121 labeled human cells (red) expressing human synaptophysin (hSYP, shown in blue) in close proximity to host DARPP32+ striatal neurons (green). e) Quantification of human synaptophysin levels in neighboring host tissue for each of the treatment groups: 2D (orange), 3D (yellow), 3DG (green), and 3DGF (purple). ** indicates $p < 0.01$ for one-way ANOVA with Dunnett's test for multiple comparisons. Absence of brackets denotes no statistical significance, with $p > 0.05$.

integration of many surviving TH+/FOXA2+ neurons may contribute to the rapid functional improvements mediated by 3DGF relative to the other treatment groups.

3. Discussion

Biomaterial platforms promise to increase the efficacy of CRT,[23,58] and incorporation of bioactive ligands into these scaffolds can promote additional important functions such as cell motility. We engineered a biologically functionalized, HA-based hydrogel, and the resulting cell transplantation platform enhanced the survival and dispersion of transplanted hESC-derived mDA neurons and resulted in the alleviation of disease symptoms in a PD rat model. The biomaterial platform developed here may also enhance the efficacy of cell types other than mDA neurons, such as medium spiny neurons or oligodendrocyte precursor cells (OPCs). Post-transplantation survival or dispersion of non-neuronal cells such as

OPCs could be similarly enhanced using the appropriate encapsulated factors.

Identification and enhancement of graft properties that alleviate disease symptoms can enable better transplantation strategies.[11] For PD therapy, to date the number of surviving TH+ cells has been among the most important criteria for graft success.[11] In addition, extensive innervation of host tissue has also recently been identified as an important factor for achieving functional recovery.[17] Graft spreading is also beneficial, as local hotspots of TH+ grafts have led to movement disorders such as dyskinesias.[19] Here, we observed both robust TH+ cell survival and dispersion, evidence for synapse formation with surrounding host neurons, and behavioral recovery. To correlate the observed trends in behavior with the various histological parameters, we plotted the data from each behavior test against each histological measure for every animal for statistical assessment (Figure S14, Supporting Information). Generally, the overall number of grafted cells, TH+ cells, and dispersion all correlated with reduced apomorphine and amphetamine-induced
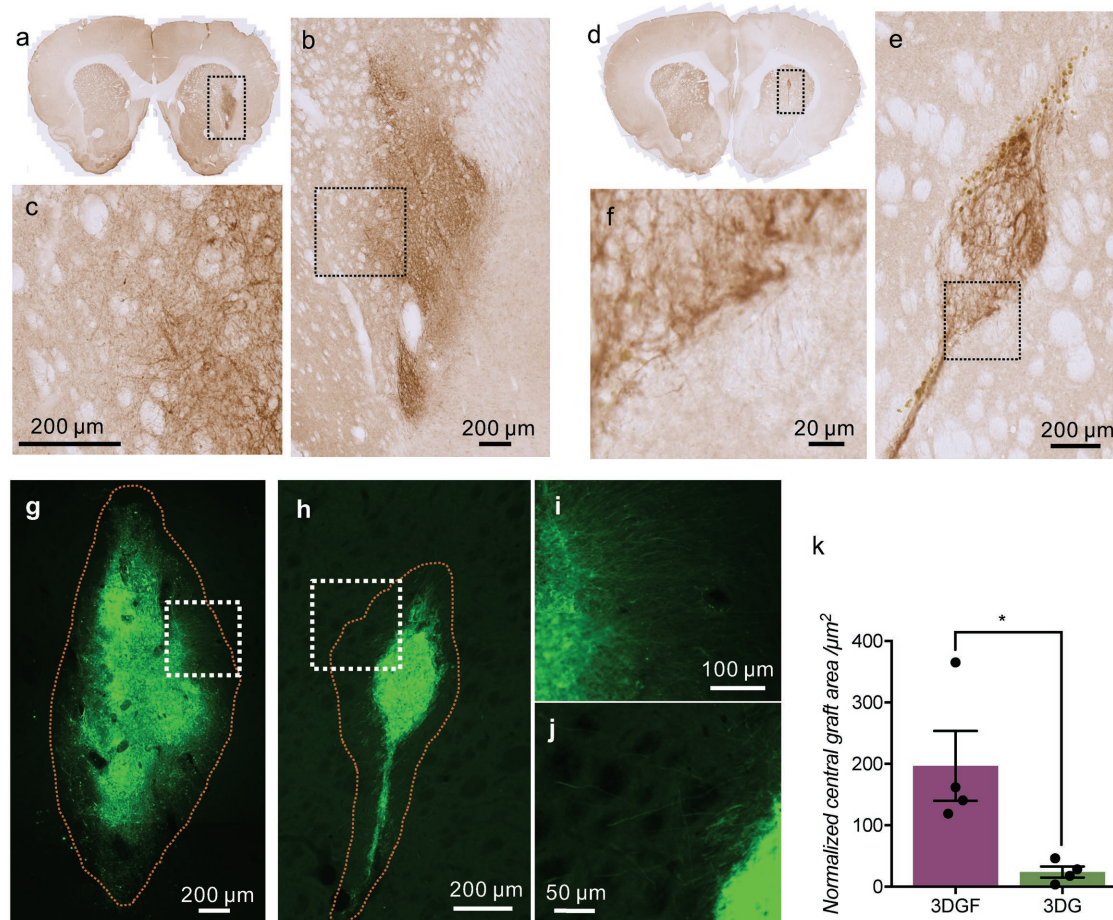
**ADVANCED
SCIENCE NEWS**

www.advancedsciencenews.com

**ADVANCED
FUNCTIONAL
MATERIALS**

www.afm-journal.de

Figure 6. Dispersion factors mediate increased neurite outgrowth and graft innervation at 20 weeks postimplantation. a) Representative brain section showing NCAM-DAB stained striatal 3DGF graft; b) inset from (a) showing full graft; c) inset from (b), showing dense innervation at the graft periphery. d) Representative brain section showing NCAM-DAB stained striatal 3DG graft; e) inset from (d) showing the full graft; f) inset from (f) showing limited innervation with few neurites at the graft periphery. Representative image showing STEM121 stained graft for g) 3DGF or h) 3DG graft. i) Inset from (g) showing high density of neurites extending >300 µm from the 3DGF graft periphery. j) Inset from (h) showing sparse neurite outgrowth from the 3DG graft. k) Quantification of total innervated area at the graft center from STEM121 stained sections, normalized to the total number of surviving cells. Data are presented as mean ± SEM for $n = 4$ animals/group. * indicates $p < 0.05$ for Student's unpaired t-test.

rotations as well as increased use of the contralateral forelimb. Interestingly, on average behavioral improvement correlated most with the level of dispersion ($R^2 = 0.22$), followed by the number of surviving TH$^+$ cells ($R^2 = 0.15$). Future preclinical experiments with larger cohorts of animals may further validate the interesting trends noted here.

CRT strategies that provide rapid treatment benefits following transplantation will be especially attractive for clinical translation. Typically for PD patients, treatment benefits from CRT are only noticeable at ten months to two years or longer after transplantation.[21,22] This slow onset is mirrored in preclinical models, where animals show significant behavioral or motor improvements starting several months post-transplantation,[10,47,48] and one potential cause is that transplanted stem or progenitor cells likely need to mature further into functional mDA neurons in vivo before producing dopamine and connecting to surrounding neurons. Here, encapsulation within a HA-based scaffold functionalized with neurotrophic and dispersive factors mediated survival, dispersion, and integration of

3D-generated mDA neurons that were transplanted at a higher level of maturity relative to neurons commonly generated on 2D.[24] That is, the combination of factors, material, and postmitotic neurons mediated faster alleviation of disease symptoms in this PD animal model (Table S3, Supporting Information).

A mechanistic understanding of the dispersion phenomenon demonstrated here may benefit future applications of this strategy. We found that HGF, Ephrin-B2, and GDNF dispersed hESC-derived mDA neurons in vitro and in vivo. HGF may promote neuronal migration in general through binding c-MET,[25] a receptor expressed in mDA neurons.[59] Likewise, GDNF likely promotes neuronal outgrowth and migration through GFRα1,[28] again a receptor reportedly expressed on mDA neurons.[59,60] However, while Ephrin-B2 in soluble form may promote neurite outgrowth,[61] and while ephrin ligands in general are known for roles in short-range axon repulsion,[62] its dispersive effect has not been noted previously and warrants further investigation. Additionally, GDNF has been strongly linked to mDA neuronal survival,[62] and Ephrin-B2

and GDNF have been associated with axonogenesis.[27,63] The combinatorial dispersive, axonogenic, and survival activities of these factors may thus have enhanced the post-transplantation fate of grafted cells. Additional candidate or unbiased screens may identify other proteins, peptides, or small molecules that could further enhance the dispersive effect.

Immunosuppression, though routinely used with CRT in the clinic, has long been a topic of debate.[64] While some preclinical studies demonstrate long-term immunosuppression to be indispensable for graft survival,[64] others find it unnecessary.[65] In support of the latter point of view, in our experiments, we did not find post-transplantation cell survival to be affected by the duration of immunosuppression (Figure S15, Supporting Information). Notably, some studies have reported that prolonged immunosuppression[66] leaves the host vulnerable to side effects including organ malfunction[67] and opportunistic infections.[68] Thus, strategies to enhance graft survival without prolonged immunosuppression may be beneficial.

We noted improvements in motor function for 3DGF-grafted PD rats (Figure 3), which correlated not only with high levels of synaptic integration (Figure 5), but perhaps most importantly, also with significantly higher levels of innervation (Figure 6). Neurite extension and innervation may be further enhanced in the future by exploring a larger parameter space (e.g., initial scaffold stiffness, scaffold degradation rate, amount and duration of factor release) when constructing the transplantation scaffold. The modular platform design utilized here could enable exploration of additional parameters including functionalities such as degradable linkers for enhanced scaffold biodegradability[69] or thermoresponsive polymer components for in situ gelation.[70] Furthermore, long-term, tunable factor release from coencapsulated microparticles may enable a persistent dispersive, survival, and axonogenic effect.[71] A more degradable scaffold and a longer-term supply of dispersion and axonogenic cues may especially enhance host-tissue innervation. By demonstrating that an engineered material can enhance treatment efficacy, this work sets a precedent for such future research.

In conclusion, we have developed a transplantation strategy to enhance cell replacement therapy for PD. Transplantation of hESC-derived mDA neurons coencapsulated with dispersion factors in optimized cell-instructive HA-based hydrogels significantly improved treatment and alleviated disease symptoms in a PD rat model. These outcomes correlated with neuron survival, innervation, and graft dispersion. This engineered material may in general advance clinical translation of regenerative medicine for degenerative disorders or trauma.

4. Experimental Section

hESC Culture and Differentiation: H1 hESCs were cultured on Matrigel (Corning) coated surfaces using supplemented E8 medium (Invitrogen), or in 3D PNIPAAm-PEG hydrogels (Mebiol; Cosmobio) using supplemented E8 medium and ROCK inhibitor (10 × 10⁻⁶ M) (Selleckem), as previously described.[24] Cells were differentiated to mDA neurons using previously established dual SMAD inhibition protocols,[10,47] on Matrigel surfaces or as encapsulated in Mebiol.[24]

Immunocytochemistry: Immunocytochemistry was performed as previously described.[24] Briefly, cells were washed with 1× PBS and fixed with paraformaldehyde (PFA) (4%) (MilliporeSigma) for 15 min at room temperature (RT). Cells were then blocked with bovine serum albumin (BSA) (2%) and donkey serum (5%) and Triton X 100 (0.1 w/v%) (MilliporeSigma), and stained with primary antibody solution overnight (on 2D) or for 48 h (in 3D hydrogels) at 4 °C with gentle rocking. Cells were then washed with 1× PBS, and incubated with secondary antibody solution for 2–4 h at RT with gentle rocking. Antibodies were used as listed in Table S1 (Supporting Information). Images were taken using a Zeiss AxioObserver fluorescent microscope, or a Zeiss LSM710 confocal microscope.

HA hydrogels: Hyaluronic acid (Lifecore Biomedical) and heparin (MilliporeSigma) were functionalized with dibenzocyclocyne (DBCO, Sigma) using EDC-NHS (MilliporeSigma) chemistry as previously described.[72] Azide-modified RGD (0.5 × 10⁻³ M) containing peptide (Azide-KGSGRGDSP, Genscript) and heparin-DBCO (0.07 w/v%) was incorporated with HA-DBCO. For cell encapsulation, hESC-derived mDA neurons were mixed with the HA formulation and rapid, bio-orthogonal gelation initiated with PEG-diazide (0.07 mol% of HA-DBCO) (Creative Pegworks) using strain-promoted azide–alkyne cycloaddition (SPAAC).[73] For factor incorporation, dispersion factors at the appropriate concentrations were mixed with the HA formulation, with or without cells, before gelation with PEG-diazide. To attain gels of differing stiffness, the HA-DBCO weight fraction was varied within the gel formulations. The shear and loss moduli of resulting gels were measured using oscillatory shear rheology on a rheometer (Anton-Parr).[74]

Release Kinetics: HA gels with incorporated GDNF, HGF, and Ephrin-B2 were seeded in 24-well transwells in a 24-well plate immediately after initiation of gelation by adding PEG-diazide. After incubating for 10 min at 37 °C to ensure complete gelation (although gelation was typically complete in <5 min at RT), one wash was performed with 1 mL 1× PBS with BSA (0.1%) to remove free, unencapsulated factors, followed by a second 5 min wash with 1× PBS (1 mL) with BSA (0.1%). The factor-loaded gel was then incubated with 1× PBS (1 mL) with BSA (0.1%) (200 µL on the gel, and 800 µL in the bottom compartment) at 37 °C. At predesignated time-points, the solution was completely removed and replenished with fresh 1× PBS with BSA (0.1%). To reduce evaporation, 1× PBS was added to surrounding wells and the plate was parafilm-wrapped. Collected supernatant at each time-point was stored at −20 °C.

Subsequently, ELISA was performed to determine the amount of factors released over time. Toward this end, first Maxisorb plates were coated overnight with gentle rocking on an orbital shaker at 4 °C with the appropriate capture antibodies at the following concentrations in 1× PBS: for HGF, anti-HGF MAB694 (2 µg mL⁻¹) (R&D systems), for GDNF, anti-GDNF MAB212 (2 µg mL⁻¹) (R&D systems), and for Ephrin-B2, anti-His antibody MA121315 (1 µg mL⁻¹) (Fisher). Next, wells were blocked with BSA (5 w/v%) in 1× PBS (300 µL) for 2 h at RT with gentle rocking. Wells were then washed three times with Tween-20 (0.05 v/v%) (Fisher) in 1× PBS (300 µL) (PBST) for 5 min each at RT with gentle rocking. Subsequently, to generate the standard curves for absorbance versus protein concentration, the relevant protein (HGF, GDNF, or Ephrin-B2) in 1× PBS (100 µL) with BSA (0.1%) was added at the appropriate concentration, or to quantify released proteins in the supernatant, the supernatant solution (100 µL) was added. Protein standards or supernatant was incubated for 2 h at RT with gentle rocking, followed by three 5 min washes with PBST. Next, the appropriate detection antibodies in 1× PBS—biotinylated goat IgG BAF294 (R&D system) (100 µL, 0.1 µg mL⁻¹) for HGF, biotinylated goat IgG BAF212 (R&D systems) (100 µL, 0.1 µg mL⁻¹) for GDNF, and rabbit anti-Ephrin-B2 sc-15397 (Santa Cruz Biotechnology) (100 µL, 0.2 µg mL⁻¹) for Ephrin-B2—was added for a 2 h incubation at RT with gentle rocking, followed by three 5 min washes with PBST. For Ephrin-B2 detection, the wells were next incubated with biotinylated goat anti-rabbit antibody 111-065-003 (Jackson) (100 µL, 0.1 µg mL⁻¹) in 1× PBS for 2 h at RT with gentle rocking, followed by three 5 min washes. Next, wells were incubated with HRP-streptavidin (Invitrogen) (100 µL at a 1:10 000 dilution) in 1× PBS for 30 min at RT with gentle rocking,

**ADVANCED
SCIENCE NEWS**

www.advancedsciencenews.com

**ADVANCED
FUNCTIONAL
MATERIALS**

www.afm-journal.de

followed by three 5 min washes. Finally, following a 10 min incubation with 3,3′,5,5′-trimethylbenzidine (TMB) (MilliporeSigma) (100 μL) at RT with gentle rocking protected from light, the absorbance at 630 nm was measured using a spectrophotometer. Alternatively, the reaction may be quenched with sulfuric acid (MilliporeSigma) (100 μL, 0.1 N) and the absorbance measured at 450 nm.

Dispersion: For dispersion on 2D, D25 hESC-derived mDA neurons generated in Mebiol (Cosmobio) were harvested and seeded on culture wells coated with laminin (20 μg mL^{-1}) (Invitrogen). mDA neuronal cultures at this stage were fed with Neurobasal medium (Invitrogen), supplemented with B27 (1:50) (Invitrogen) and Glutamax (1:100) (Invitrogen). For dispersion in 3D, D25 hESC-derived mDA neurons generated in Mebiol (Cosmobio) were harvested and seeded in HA hydrogels. 2 d postseeding, appropriate dispersion molecules were introduced at the following concentrations that are similar to values in previous work: HGF (Peprotech) (20 ng mL^{-1}),[25] FGF-2 (Peprotech) (20 ng mL^{-1}),[26] Ephrin B1 (produced as previously described[75]) (10 ng mL^{-1}), Ephrin-B2 (produced as previously described[75]) (10 ng mL^{-1}), and GDNF (Peprotech) (100 ng mL^{-1}).[28] For the controlled release 3D gels, D25 hESC-derived mDA neurons were encapsulated in HA gels with the appropriate amount of dispersion factors (1 μg GDNF, 0.5 μg Ephrin-B2, and 0.5 μg HGF in a 30 μL HA gel). At predetermined time-points cells were fixed, stained for immunocytochemistry and imaged using a Zeiss AxioObserver fluorescent microscope for 2D, or using a Zeiss LSM710 confocal microscope for 3D.

To assess the effect of dispersion factors on total cell numbers, D25 hESC-derived mDA neurons seeded on laminin-coated surfaces were treated with GDNF (100 ng mL^{-1}), EphrinB2 (10 ng mL^{-1}), HGF (20 ng mL^{-1}), or all three factors in combination.

For quantification of dispersion, images were analyzed using a customized workflow using modules in Cell Profiler software (cellprofiler.org). Briefly, cell nuclei in images were identified using "Identify primary objects" module, and subsequently internuclear distances were measured using "Measure object neighbor" module (Figure S1, Supporting Information).

Voltage-Sensitive Dye-Based Imaging: D31 H1 hESC-derived mDA neurons generated in pNIPAAm-PEG hydrogels and seeded on laminin-coated coverslips were labeled with voltage-sensitive dyes dsVF2.2(OMe).Cl (500 × 10^{-9} M),[57] and images were acquired with a W-Plan-Apo 63×/1.0 objective (Zeiss) and OrcaFlash4.0 sCMOS camera (sCMOS, Hamamatsu) and analyzed as previously described.[76]

In Vivo Transplantation: All stem cell procedures and procedures in animals were performed following NIH guidelines for animal care and use and were approved by the UC Berkeley Animal Care and Use Committee (ACUC), the Committee for Laboratory and Environmental Biosafety (CLEB), and the Stem Cell Research Oversight committee (SCRO).

Prior to transplantation, 6-OHDA unilesioned Sprague-Dawley rats (Charles River) were assessed using apomorphine-induced contralateral rotation as described below. Only rats that demonstrated on average >6 net ipsilateral rotations min^{-1} for at least 50 min were used in the study.

H1 hESCs were differentiated to mDA neurons on Matrigel-coated surfaces or in 3D PNIPAAm-PEG hydrogels for 25 d. Cells were then harvested from each platform using ice-cold PBS and pipet mixed to generate small clusters (50–100 μm sized). Cells were centrifuged and resuspended in B27 supplemented Neurobasal medium (2D and 3D groups), in HA hydrogels functionalized with RGD and heparin (3D gel group), or in HA hydrogels functionalized with RGD, heparin, and dispersion factors (3D gel+factors group) at 20 000 cells μL^{-1}. Immediately before loading the injection needle with hydrogel-encapsulated cells prior to implantation, PEG-diazide was added to initiate gelation. Cells (100 000 in 5 μL) were implanted into the striatum of isoflurane anesthetized 200–250 g adult female 6-OHDA unilesioned Sprague-Dawley rats (Charles River) (at stereotaxic coordinates AP: +1.0, ML: −2.5, DV: −5.0) at a manually controlled injection rate (1 μL min^{-1}) using a 10 μL syringe with a 22s Gauge Point Style 4 needle with a 30° angle (Hamilton).

As controls, PBS (sham group) or HA hydrogels functionalized with RGD, heparin, and dispersion factors (gel group) were used. Six animals were assigned per group. Cyclosporine (10 mg kg^{-1}) was injected intraperitoneally daily starting 24 h before surgeries and until four weeks post-transplantation.

Behavior Assays: Motor function in rats was monitored using a standard battery of tests which included apomorphine-induced rotation,[51] amphetamine-induced rotation,[53] cylinder test for forelimb akinesia,[52] and stepping test for forelimb akinesia[54] as previously described, in a double-blind manner. Apomorphine-induced rotation and cylinder test for forelimb akinesia were performed starting one week before transplantations, and subsequently once every month for five months post-transplantation. Amphetamine-induced rotation and stepping test for forelimb akinesia were performed five months post-transplantation. Briefly, apomorphine (0.05 mg kg^{-1}) (MilliporeSigma) in deionized (DI) water with sodium metabisulfite (0.1 w/v%) (MilliporeSigma) was injected intraperitoneally, and net contralateral rotations recorded for 60 min using a Rotometer and Fusion software (Omnitech). Similarly, for amphetamine-induced rotations, amphetamine (5 mg kg^{-1}) (MilliporeSigma) in DI water was injected intraperitoneally, and net ipsilateral rotations quantified for 90 min using a Rotometer and Fusion software (Omnitech). For the cylinder test, rats were placed in tall, transparent cylinders and allowed to freely explore, and the number of weight-bearing right or left forepaw touches to the sides of the cylinder were recorded for 15 min, or until 30 total forepaw touches. For the stepping test, rats with hindlimbs manually restrained were gently dragged across a 1 m flat surface in ≈20 s, in alternating forward and reverse directions for a total of six trials per animal, and the number of right and left forepaw touches recorded. Researchers recording the behavior data were blind to the identity of the treatment groups at all times.

Immunohistochemistry: Five months after cell implantations, animals were transcardially perfused with 4% PFA (MilliporeSigma). Brains were harvested and incubated in 4% PFA (MilliporeSigma) overnight, and transferred into a 30% (w/v) sucrose (MilliporeSigma) solution the following day.

After sufficient dehydration, brains were sliced into sections (40 μm thick) using a freezing microtome. Primary antibodies diluted in primary blocking buffer (5% donkey serum, 2% BSA, 0.1% Triton X 100 (MilliporeSigma)) at concentrations listed in Table S2 (Supporting Information) were incubated with the brain sections for 72 h with gentle rocking at 4 °C. Following incubation, brain sections were rinsed once with Triton (0.2%) in PBS and washed three times with Triton (0.1%) in PBS, followed by a 4 h incubation with appropriate secondary antibodies diluted in PBS with BSA (0.2%). 4,6-diamidino-2-phenylindole (DAPI) was added 30 min before the end of secondary antibody incubation period. Brain sections were subsequently washed with PBS and mounted. A Zeiss Axioscan Z1 automated slide scanner, a Zeiss AxioObserver fluorescent microscope, and a Zeiss LSM710 confocal microscope were used for imaging, and Zen 2.0 software or ImageJ was used for analysis.

For TH-DAB and NCAM-DAB staining, 40 μm sections were washed three times in TBST (0.05% v/v Tween20 in Tris-buffered saline) with gentle rocking. Sections were then treated with Triton X (0.1%) and hydrogen peroxide (0.6%) in TBST for 40 min at room temperature. Subsequently, following three washes in TBST, sections were blocked in goat serum (10%) for 1 h at room temperature, followed by an overnight incubation at 4 °C with rabbit primary antibodies diluted in TBST with goat serum (1%). The next day, sections were washed four times in TBST, and then incubated for 1 h with biotinylated goat-anti-rabbit secondary antibody (Jackson Immunolabs) diluted in TBST with 1% goat serum. Sections were then washed four times with TBST, and incubated with ABC solution (Vector Laboratories) for 40 min at room temperature. Next, sections were washed four times with TBST and once with Tris (0.1 M pH 7.4). 3,3′-Diaminobenzidine (DAB) (MilliporeSigma) in Tris (0.1 M, pH 7.4) was used to stain sections for 5 min, followed by four washes in Tris (0.1 M, pH 7.4). Sections were then mounted on slides, and dried overnight. The next day, mounted slides were cleaned by dipping in Citrisolv (Thermofisher Scientific), dried, and cover-slipped

with Entellan (MilliporeSigma). A Zeiss Axioscan Z1 automated slide scanner was used for imaging, and Zen 2.0 software was used for analysis.

The percentage of cell survival was quantified using the cell counter feature on ImageJ, following Abercrombie's method as previously described.[77] All cells positive for HNA and TH were counted from zoomed-in pictures originally acquired at 5× magnification on the Zeiss Axioscan slide scanner, of every fifth brain section spanning the injection site (≈8 sections across ≈50 total sections). The total number of HNA and TH positive cells were then extrapolated from these counts. Furthermore, all HNA positive cells were counted from three representative sections for each rat brain, and imaged at 20× magnification on the Zeiss AxiObserver. Cells double positive for TH/HNA and FOXA2/HNA were then quantified in these images.

Average fluorescence intensity from human synaptophysin expression in regions of interest within the grafts or in peripheral host tissues was quantified in ImageJ. Representative images from at least four different animals for each of the treatment groups were used in the quantification.

Graft dispersion was quantified using the Cell Profiler workflow, as described above, on representative images of HNA⁺ grafts from all animals in each treatment group.

Innervation in the 3DGF and 3DG groups was quantified by measuring the total area covered by human neurites in the rat striatum at the coronally central graft section. Representative images from four different animals for each group were used in the quantification.

Statistics: All statistics were performed using Prism software (GraphPad). In Figure 1e, dispersion was analyzed using two-tailed unpaired *t*-test. All other analyses were performed using one-way ANOVA with Tukey's test for multiple comparisons, or Dunnet's test for multiple comparison for select groups.

There are no data with mandated deposition.

Supporting Information

Supporting Information is available from the Wiley Online Library or from the author.

Conflict of Interest

The authors declare that Maroof Adil, Sanjay Kumar and David Schaffer are co-inventors on a pending patent application related to transplantable HA-based biomaterials.

[1]   L. V. Kalia, A. E. Lang, *Lancet* **2015**, *386*, 896.
[2]   S. L. Kowal, T. M. Dall, R. Chakrabarti, M. V. Storm, A. Jain, *Mov. Disord.* **2013**, *28*, 311.
[3]   O. Lindvall, A. Björklund, *NeuroRx* **2004**, *1*, 379.
[4]   C. R. Freed, R. E. Breeze, N. L. Rosenberg, S. A. Schnek, E. Kriek, J.-X. Qi, T. Lone, Y.-B. Zhang, J. A. Snyder, T. H. Wells, L. O. Ramig, L. Thompson, J. C. Mazziotta, S. Huang, S. T. Grafton, D. Brooks, G. Sawle, G. Schroter, A. A. Ansari, *N. Engl. J. Med.* **1992**, *327*, 1549.
[5]   H. Widner, J. Tetrud, S. Rehncrona, B. Snow, P. Brundin, B. Gustavil, A. Bjorklund, O. Lindvall, J. W. Langston, *N. Engl. J. Med.* **1992**, *327*, 1556.
[6]   D. D. Spencer, R. J. Robbins, F. Naftolin, K. L. Marek, T. Vollmer, C. Leranth, R. H. Roth, L. H. Price, A. Gjedde, B. S. Bunney, K. J. Sass, J. D. Elsworth, E. L. Kier, R. Makuch, P. B. Hoffer, D. E. Redmond Jr., *N. Engl. J. Med.* **1992**, *327*, 1541.
[7]   R. A. Barker, J. Barrett, S. L. Mason, A. Björklund, *Lancet Neurol.* **2013**, *12*, 84.
[8]   M. Politis, K. Wu, C. Loane, N. P. Quinn, D. J. Brooks, S. Rehncrona, A. Bjorklund, O. Lindvall, P. Piccini, *Sci. Transl. Med.* **2010**, *2*, 38ra46.
[9]   V. Tabar, L. Studer, *Nat. Rev. Genet.* **2014**, *15*, 82.
[10] S. Kriks, J.-W. Shim, J. Piao, Y. M. Ganat, D. R. Wakeman, Z. Xie, L. Carrillo-Reid, G. Auyeung, C. Antonacci, A. Buch, L. Yang, M. F. Beal, D. J. Surmeier, J. H. Kordower, V. Tabar, L. Studer, *Nature* **2011**, *480*, 547.
[11] A. Kirkeby, S. Nolbrant, K. Tiklova, A. Heuer, N. Kee, T. Cardoso, D. R. Ottosson, M. J. Lelos, P. Rifes, S. B. Dunnett, S. Grealish, T. Perlmann, M. Parmar, *Cell Stem Cell* **2017**, *20*, 1.
[12] R. A. Barker, *Cell Stem Cell* **2014**, *15*, 539.
[13] R. A. Barker, M. Parmar, A. Kirkeby, A. Björklund, L. Thompson, P. Brundin, *J. Parkinson's Dis.* **2016**, *6*, 57.
[14] Y. M. Ganat, E. L. Calder, S. Kriks, J. Nelander, E. Y. Tu, F. Jia, D. Battista, N. Harrison, M. Parmar, M. J. Tomishima, *J. Clin. Invest.* **2012**, *122*, 2928.
[15] J. C. Niclis, C. W. Gantner, C. P. J. Hunt, J. A. Kauhausen, J. C. Durnall, J. M. Haynes, C. W. Pouton, C. L. Parish, L. H. Thompson, *Stem Cell Rep.* **2017**, *9*, 868.
[16] B. A. Aguado, W. Mulyasasmita, J. Su, K. J. Lampe, S. C. Heilshorn, *Tissue Eng., Part A* **2012**, *18*, 806.
[17] J. A. Steinbeck, S. J. Choi, A. Mrejeru, Y. Ganat, K. Deisseroth, D. Sulzer, E. V Mosharov, L. Studer, *Nat. Biotechnol.* **2015**, *33*, 204.
[18] Y. Ma, A. Feigin, V. Dhawan, M. Fukuda, Q. Shi, P. Greene, R. Breeze, S. Fahn, C. Freed, D. Eidelberg, *Ann. Neurol.* **2002**, *52*, 628.
[19] E. Maries, J. H. Kordower, Y. Chu, T. J. Collier, C. E. Sortwell, E. Olaru, K. Shannon, K. Steece-Collier, *Neurobiol. Dis.* **2006**, *21*, 165.
[20] H. Ghashghaei, C. Lai, E. S. Anton, *Nat. Rev. Neurosci.* **2007**, *8*, 141.
[21] W. Li, E. Englund, H. Widner, B. Mattsson, D. van Westen, J. Lätt, S. Rehncrona, P. Brundin, A. Björklund, O. Lindvall, J.-Y. Li, *Proc. Natl. Acad. Sci. USA* **2016**, *113*, 6544.
[22] P. Hagell, P. Brundin, *J. Neuropathol. Exp. Neurol.* **2001**, *60*, 741.
[23] J. A. Burdick, R. L. Mauck, S. Gerecht, *Cell Stem Cell* **2016**, *18*, 13.
[24] M. M. Adil, G. M. Rodrigues, R. U. Kulkarni, A. T. Rao, N. E. Chernavsky, E. W. Miller, D. V. Schaffer, *Sci. Rep.* **2017**, *7*, 40573.

[25] E. M. Powell, W. M. Mars, P. Levitt, *Neuroendocrinology* **2001**, *30*, 79.

[26] T. C. Lim, S. Rokkappanavar, W. S. Toh, L.-S. Wang, M. Kurisawa, M. Spector, *FASEB J.* **2013**, *27*, 1023.

[27] J. Rodger, L. Salvatore, P. Migani, *NeuroSignals* **2012**, *20*, 190.

[28] E. Pozas, C. F. Ibáñez, *Neuroendocrinology* **2005**, *45*, 701.

[29] M. Tessier-Lavigne, C. S. Goodman, *Science* **1996**, *274*, 1123.

[30] R. Kittappa, W. W. Chang, R. B. Awatramani, R. D. G. McKay, *PLoS Biol.* **2007**, *5*, e325.

[31] A. Pristerà, W. Lin, A.-K. Kaufmann, K. R. Brimblecombe, S. Threlfell, P. D. Dodson, P. J. Magill, C. Fernandes, S. J. Cragg, S.-L. Ang, *Proc. Natl. Acad. Sci. USA* **2015**, *112*, E4929.

[32] J. A. Burdick, G. D. Prestwich, *Adv. Mater.* **2011**, *23*, H41.

[33] M. M. Adil, T. Vazin, B. Ananthanarayanan, G. M. Rodrigues, A. T. Rao, R. U. Kulkarni, E. W. Miller, S. Kumar, D. V. Schaffer, *Biomaterials* **2017**, *136*, 1.

[34] U. Hersel, C. Dahmen, H. Kessler, *Biomaterials* **2003**, *24*, 4385.

[35] X. d'Anglemont de Tassigny, A. Pascual, J. López-Barneo, *Front. Neuroanat.* **2015**, *9*, 10.

[36] Z. C. Baquet, P. C. Bickford, K. R. Jones, *J. Neurosci.* **2005**, *25*, 6251.

[37] M. Timmer, K. Cesnulevicius, C. Winkler, J. Kolb, E. Lipokatic-Takacs, J. Jungnickel, C. Grothe, *J. Neurosci.* **2007**, *27*, 459.

[38] S. E. Sakiyama-Elbert, *Acta Biomater.* **2014**, *10*, 1581.

[39] M. R. Ng, A. Besser, G. Danuser, J. S. Brugge, *J. Cell Biol.* **2012**, *199*, 545.

[40] A. D. Doyle, N. Carvajal, A. Jin, K. Matsumoto, K. M. Yamada, *Nat. Commun.* **2015**, *6*, 8720.

[41] E. Gherardi, D. Y. Chirgadze, J. P. Hepple, H. Zhou, R. A. Byrd, T. L. Blundell, *Nat. Struct. Biol.* **1999**, *6*, 72.

[42] J.-P. Himanen, K. R. Rajashankar, M. Lackmann, C. A. Cowan, M. Henkemeyer, D. B. Nikolov, *Nature* **2001**, *414*, 933.

[43] C. Eigenbrot, N. Gerber, *Nat. Struct. Biol.* **1997**, *4*, 435.

[44] M. M. Pakulska, I. E. Donaghue, J. M. Obermeyer, A. Tuladhar, C. K. McLaughlin, T. N. Shendruk, M. S. Shoichet, *Sci. Adv.* **2016**, *2*, e1600519.

[45] K. Mizuno, H. Inoue, M. Hagiya, S. Shimizu, T. Nose, Y. Shimohigashi, T. Nakamura, *J. Biol. Chem.* **1994**, *269*, 1131.

[46] M. Tanaka, H. Xiao, K. Kiuchi, *Neuroreport* **2002**, *13*, 1913.

[47] A. Kirkeby, S. Grealish, D. A. Wolf, J. Nelander, J. Wood, M. Lundblad, O. Lindvall, M. Parmar, *Cell Rep.* **2012**, *1*, 703.

[48] S. Grealish, E. Diguet, A. Kirkeby, B. Mattsson, A. Heuer, Y. Bramoulle, N. Van Camp, A. L. Perrier, P. Hantraye, A. Björklund, M. Parmar, *Cell Stem Cell* **2014**, *15*, 653.

[49] D. Doi, B. Samata, M. Katsukawa, T. Kikuchi, A. Morizane, Y. Ono, K. Sekiguchi, M. Nakagawa, M. Parmar, J. Takahashi, *Stem Cell Rep.* **2014**, *2*, 337.

[50] D. R. Wakeman, B. M. Hiller, D. J. Marmion, C. W. Mcmahon, G. T. Corbett, K. P. Mangan, J. Ma, L. E. Little, Z. Xie, T. Perez-rosello, J. N. Guzman, D. J. Surmeier, J. H. Kordower, *Stem Cell Rep.* **2017**, *9*, 149.

[51] F. Hefti, E. Melamed, R. J. Wurtman, *Brain Res.* **1980**, *195*, 123.

[52] T. Schallert, S. Fleming, J. Leasure, J. Tillerson, S. Bland, *Neuropharmacology* **2000**, *39*, 777.

[53] U. Ungerstedt, G. W. Arbuthnott, *Brain Res.* **1970**, *24*, 485.

[54] M. Olsson, G. Nikkhah, C. Bentlage, A. Björklund, *J. Neurosci.* **1995**, *15*, 3863.

[55] P. Voorn, L. J. M. J. Vanderschuren, H. J. Groenewegen, T. W. Robbins, C. M. A. Pennartz, *Trends Neurosci.* **2004**, *27*, 468.

[56] M. Onorati, V. Castiglioni, D. Biasci, E. Cesana, R. Menon, R. Vuono, F. Talpo, R. L. Goya, P. A. Lyons, G. P. Bulfamante, L. Muzio, G. Martino, M. Toselli, C. Farina, R. A. Barker, G. Biella, E. Cattaneo, *Nat. Neurosci.* **2014**, *17*, 1.

[57] R. U. Kulkarni, H. Yin, N. Pourmandi, F. James, M. M. Adil, D. V. Schaffer, Y. Wang, E. W. Miller, *ACS Chem. Biol.* **2017**, *12*, 407.

[58] C. Qi, X. Yan, C. Huang, A. Melerzanov, Y. Du, *Protein Cell* **2015**, *6*, 638.

[59] X. Zeng, J. Cai, J. Chen, Y. Luo, Z. You, E. Fotter, Y. Wang, B. Harvey, T. Miura, C. Backman, G. Chen, M. S. Rao, J. Freed, *Stem Cells* **2004**, *22*, 925.

[60] C. R. Bye, M. E. Jönsson, A. Björklund, C. L. Parish, L. H. Thompson, *Proc. Natl. Acad. Sci. USA* **2015**, *112*, E1946.

[61] Y. Yue, D. A. J. Widmer, A. K. Halladay, D. P. Cerretti, G. C. Wagner, J. Dreyer, R. Zhou, *J. Neurosci.* **1999**, *19*, 2090.

[62] A. Pascual, M. Hidalgo-Figueroa, J. I. Piruat, C. O. Pintado, R. Gómez-Díaz, J. López-Barneo, *Nat. Neurosci.* **2008**, *11*, 755.

[63] L. F. Lin, D. H. Doherty, J. D. Lile, S. Bektesh, F. Collins, *Science* **1993**, *260*, 1130 LP.

[64] A. L. Piquet, K. Venkiteswaran, N. I. Marupudi, M. Berk, T. Subramanian, *Brain Res. Bull.* **2012**, *88*, 320.

[65] H. Widner, P. Brundin, *Cell Transplant.* **1993**, *2*, 307.

[66] C. Winkler, D. Kirik, A. Björklund, *Trends Neurosci.* **2005**, *28*, 86.

[67] R. Rezzani, *Prog. Histochem. Cytochem.* **2004**, *39*, 85.

[68] M. M. López, J. E. Valenzuela, F. C. Álvarez, M. R. López-Álvarez, G. S. Cecilia, P. P. Paricio, *Transpl. Immunol.* **2006**, *17*, 31.

[69] G. D. Nicodemus, S. J. Bryant, *Tissue Eng., Part B* **2008**, *14*, 149.

[70] E. Ruel-Gariépy, J. C. Leroux, *Eur. J. Pharm. Biopharm.* **2004**, *58*, 409.

[71] K. Fu, A. M. Klibanov, R. Langer, *Nat. Biotechnol.* **2000**, *18*, 24.

[72] F. A. Pelissier, J. C. Garbe, B. Ananthanarayanan, M. Miyano, C. Lin, T. Jokela, S. Kumar, M. R. Stampfer, J. B. Lorens, M. A. LaBarge, *Cell Rep.* **2014**, *7*, 1926.

[73] X. Ning, J. Guo, M. A. Wolfert, G. J. Boons, *Angew. Chem., Int. Ed.* **2008**, *47*, 2253.

[74] B. Ananthanarayanan, Y. Kim, S. Kumar, *Biomaterials* **2011**, *32*, 7913.

[75] A. Conway, T. Vazin, D. P. Spelke, N. A. Rode, K. E. Healy, R. S. Kane, D. V Schaffer, *Nat. Nannotechnol.* **2013**, *8*, 831.

[76] R. U. Kulkarni, D. J. Kramer, N. Pourmandi, K. Karbasi, H. S. Bateup, E. W. Miller, *Proc. Natl. Acad. Sci. USA* **2017**, *114*, 2813.

[77] M. Abercrombie, *Anat. Rec.* **1946**, *94*, 239.